2021-11-01

A Low-Complexity Method for Parameter Estimation of the Simplified Randles Circuit with Experimental Verification

Mitar Simić, Adrian Stavrakis, Goran Stojanović

A Low-Complexity Method for Parameter Estimation of the Simplified Randles Circuit with Experimental Verification

Mitar Simić, IEEE *Member*, Adrian K. Stavrakis, IEEE *Student Member* and Goran M. Stojanović, IEEE *Member*

***Abstract*— In this paper we present a processing-efficient method for parameter estimation of a Randles circuit. As our approach is not iterative, it does not require for an initial guess of model parameters to be provided. The low-complexity of the provided set of closed-form expressions enables the implementation on microcontroller-based platforms. The presented approach is verified with simulations (using both noiseless data and data with noise) and with experimentally obtained data (Randles circuit made from discrete components; impedance of microfluidic platform for isomalt detection; impedance of Panasonic 18650PF Li-ion Battery). Additionally, it was implemented on a microcontroller board based on ATmega2560 microcontroller with available 256 kB of flash memory, 8 kB of SRAM and clock speed of 16 MHz. Reliable and accurate estimations of such implementations confirmed the suitability of this work for low-cost embedded hardware.**

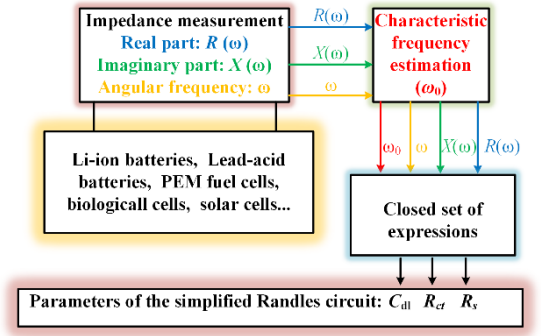

***Index Terms*— Electrical impedance spectroscopy, Randles circuit, parameter estimation, microcontroller-based platforms.**

I. Introduction

A Randles circuit topology is widely applied in the modeling of various processes and sensors [1]-[10]. For example, it was used in real-time estimation of lithium-ion [1], or lead-acid battery states [2], as well as in real time battery power capability estimation [3]. Evaluation of the ripple effects on commercial Proton-exchange membrane (PEM) fuel cell was reported in [4]. It has also been used in the characterization of different materials, such as surface microhardness of Q235 steel [5], corrosion inhibition of benzyltriethylammonium chloride [6] or assessment of interfacial characteristics of the intermetallic phases present in aluminium alloy 2024-T3 [7]. The simplified Randles circuit was also used to predict coupled mechanical, thermal, electrical and electro-chemical responses of batteries in LS-DYNA software simulations [8], which is very important for safety of large-format and energy-dense batteries used in electric vehicles. Moreover, a methodology for characterizing biological cells using a Randles circuit was investigated in [9]. Degradation of solar cells (due to various unavoidable phenomena such as thermal cycling, damp heat, exposure to ultraviolet radiation, and mechanical stress) was also analyzed by monitoring the changes in a Randles equivalent circuit parameters [10].

The parameter estimation of a Randles circuit is usually done by applying recursive non-linear least square methods and curve fitting methods. Such approaches are time-consuming and require high-end processing units [11, 12]. They are usually implemented in Personal Computer (PC) based environments. There are numerous Electrochemical Impedance Spectroscopy (EIS) software packages that can be used for parameter estimation of different equivalent circuits: Zview, ZSim, MEISP (Multiple EIS parameterization), LEVMW, EIS Spectrum, *etc.* However, if the target is the standalone use at remote locations with limited supply and processing sources, it is very important to develop methods that are not based on the aforementioned software packages.

Portable approaches are less general as they are usually optimized for a specific equivalent circuit, but they provide significant improvements in performances, such as faster execution time, with smaller power and memory needs [13,14]. Parameter estimation of a Randles circuit using system identification was reported in [15]. However, the estimation of model parameters was performed with the iterative search method, requiring sampling and processing of the input pulsating voltage and the output response current [15]. Pulsed execution was also used in time-frequency analysis and

This research was funded through the European Union's Horizon 2020 research and innovation programme under grant agreement No. 854194, and by the Ministry of Scientific and technological development, higher education and informational society of the Republic of Srpska with project "Signal Processing in Edge Computing" (Project No. 19.032/961-83/19).

Mitar Simić, Adrian K. Stavrakis and Goran M. Stojanović are with Faculty of Technical Sciences, University of Novi Sad, 21000 Novi Sad, Serbia (e-mails: mitar.simic@uns.ac.rs, sadrian@uns.ac.rs, sgoran@uns.ac.rs).

parameter estimation of a Randles circuit in [16]. The presented approach is based on the Octave/MATLAB Time-Frequency Toolbox which is not convenient for applications with embedded hardware outside the laboratory environment [16]. Therefore, a development of methods for parameter estimation of a Randles circuit in real-time with portable and low-cost hardware platforms is still an open question.

In this paper, our focus is on the development and validation of a low-complexity method for parameter estimation of the simplified Randles circuit. The input dataset includes only measured values of the complex impedance. The main contributions of our approach are: (1) elimination of the need for initial guess of model parameters, (2) non-iterative method: stable and repeatable estimation results, (3) elimination of the need for measurements at very high and very low frequencies, and (4) suitability for deployment on embedded hardware platforms which can ensure autonomous parameter estimation without the need for any external inputs or actions.

This paper is organized as follows: In section II, the structure of the simplified Randles circuit is presented. Moreover, our approach for parameter estimation is described and theoretically analyzed. Section III contains the main simulation results using synthetic noiseless data and data with noise. Section IV presents the main experimental results, including parameter estimation from measured impedance of a discrete components circuit, as well as the impedance of a microfluidic platform for isomalt detection and the impedance of Panasonic 18650PF Li-ion Battery. Section V is a conclusion with discussion regarding future works.

II. Theoretical Aspects of the Proposed Method

A. Simplified Randles Circuit

The Randles model was firstly presented in 1947 [17]. Its electrical representation is composed of two resistors (R_s and R_{ct}) and one capacitor (C_{dl}) as shown in Fig. 1. The resistor R_s represents the solution resistance, while R_{ct} models the charge transfer resistance. The double-layer structure between the electrolyte and the electrodes is taken into account with capacitor C_{dl}.

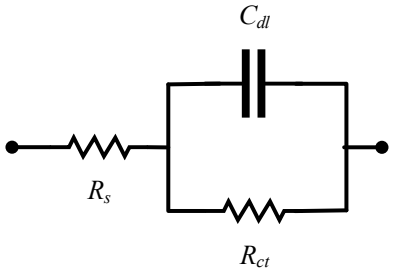

Fig. 1. Simplified Randles circuit.

The complex impedance of the circuit shown in Fig. 1 at a given angular frequency ω [rad/s] is given by Eq. (1):

$$\underline{Z}(\omega) = R(\omega) + jX(\omega) = R_s + \frac{R_{ct}}{1 + j\omega R_{ct} C_{dl}} \quad (1)$$

where $R(\omega)$ is real part (resistance) of $\underline{Z}(\omega)$, and $X(\omega)$ is imaginary part (reactance) of $\underline{Z}(\omega)$. With impedance measurement, it is possible to obtain values for $R(\omega)$ and $X(\omega)$ at a known angular frequency $\omega=2\pi f$, where f is frequency in Hz. $R(\omega)$, $X(\omega)$ and ω are usually used as input data for EIS software (Zview, ZSim, MEISP, LEVMW, EIS Spectrum, *etc.*) for the estimation of R_s, R_{ct} and C_{dl}.

B. The proposed non-iterative method for parameter estimation

The real and imaginary parts of $\underline{Z}(\omega)$ from Eq. (1) can be defined as follows:

$$R(\omega) = R_s + \frac{R_{ct}}{1 + (\omega R_{ct} C_{dl})^2} \quad (2)$$

$$X(\omega) = -\frac{\omega R_{ct}^2 C_{dl}}{1 + (\omega R_{ct} C_{dl})^2} \quad (3)$$

A typical Nyquist plot (resistance versus negative signed reactance) is shown in Fig. 2. As it can be observed, at very low frequencies (theoretically $\omega=0$), resistance is equal to the sum R_s+R_{ct}. At very high frequencies (theoretically $\omega\to\infty$), resistance is equal to the value of R_s. At the characteristic angular frequency of the Randles circuit (reciprocal value of the time constant $\tau=R_{ct}C_{dl}$.), the absolute value of the reactance has a maximum. However, an estimation of parameters from these three frequencies is not reliable in many practical applications. Reasons are: (1) need for very wide frequency span (usually from 0.001 mHz or even less, up to few or tens of MHz), (2) required time to perform low frequency measurements, (3) required complexity of such device.

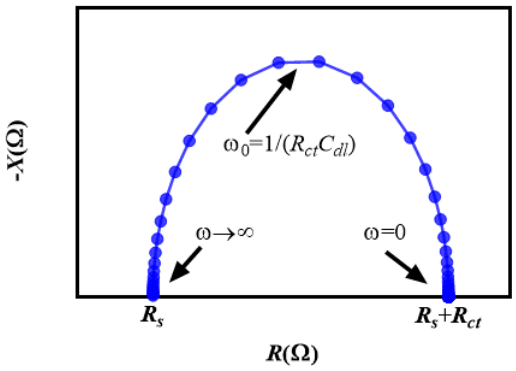

Fig. 2. Typical Nyquist plot of the Randles circuit.

First derivative of $X(\omega)$ with respect to ω is equal to zero at frequency:

$$\omega_0 = \frac{1}{R_{ct} C_{dl}} \quad (4)$$

which is also a characteristic angular frequency of the Randles circuit. As the characteristic angular frequency is equal to the angular frequency where first derivative of $X(\omega)$ is equal to zero, it means that it can be determined from measured input data $X(\omega)$ as the angular frequency where $|X(\omega)|$ presents a maximum.

Therefore, if the characteristic angular frequency ($\hat{\omega}_0$) can be accurately estimated from the measured $X(\omega)$ it can be used as a global parameter which will form a set of three input parameters ($R(\omega)$, $X(\omega)$ and $\hat{\omega}_0$) that can be used to estimate three model parameters ($\hat{R}_s(\omega_i)$, $\hat{R}_{ct}(\omega_i)$ and $\hat{C}_{dl}(\omega_i)$):

$$\hat{R}_s(\omega_i) = \frac{X(\omega_i)\cdot\hat{\omega}_0 + R(\omega_i)\cdot\omega_i}{\omega_i} \quad (5)$$

$$\hat{R}_{ct}(\omega_i) = -\frac{X(\omega_i)\cdot(\hat{\omega}_0^2+\omega_i^2)}{\omega_i\cdot\hat{\omega}_0} \quad (6)$$

$$\hat{C}_{dl}(\omega_i) = -\frac{\omega_i}{X(\omega_i)\cdot(\hat{\omega}_0^2+\omega_i^2)} \quad (7)$$

at each measurement angular frequency ω_i, where i is an integer and ranges from 1 to N, with N being the number of measurement points. The values obtained with (5)-(7) are constant if there is neither measurement noise, nor an error in characteristic frequency estimation. However, those conditions can be rarely met, so as a final step, we propose that the output values ($\hat{R}_s$,$\hat{R}_{ct}$ and $\hat{C}_{dl}$) are estimated by means of ($\hat{R}_s(\omega_i)$,$\hat{R}_{ct}(\omega_i)$ and $\hat{C}_{dl}(\omega_i)$).

C. Accuracy analysis of the proposed non-iterative method for parameter estimation

As it can be seen from (5)-(7), the estimation accuracy of the model parameters with the proposed method is directly affected by noise and/or estimation error of the characteristic frequency.

The error in the characteristic frequency estimation is directly linked to the limited number of measurement points (consequently to the frequency step). Additionally, the maximum absolute error in the estimation of characteristic frequency is equal to the half of the frequency step. In a given frequency range (f_{min}, f_{max}) a number of frequency points N defines the frequency step as:

$$\Delta f = \frac{f_{max}-f_{min}}{N-1} \quad (8)$$

That means that the relative error of characteristic frequency estimation is:

$$\delta f_c = \frac{f_{max}-f_{min}}{2\cdot f_c\cdot(N-1)} \quad (9)$$

Therefore, a proposed number of measurement points can be determined for the worst case scenario (f_c=f_{min}) and define the maximum relative error of characteristic frequency estimation (δf_c):

$$N = 1+\frac{f_{max}-f_{min}}{2\cdot f_{min}\cdot\delta f_c} \quad (10)$$

In order to determine the dependence of estimation accuracy on measurement noise and characteristic frequency estimation, it is necessary to find the first derivative of the model parameters as a functions of R, X and ω_0, as it is shown in Table I.

TABLE I
FIRST DERIVATIVES OF MODEL PARAMETERS WITH A RESPECT TO THE INPUT PARAMETERS

	R_s	R_{ct}	C_{dl}
$\frac{\partial}{\partial R}$	1	0	0
$\frac{\partial}{\partial X}$	$\frac{\hat{\omega}_0}{\omega}$	$\frac{-(\omega^2+\hat{\omega}_0^2)}{\omega\cdot\hat{\omega}_0}$	$\frac{\omega}{X^2(\omega^2+\hat{\omega}_0^2)}$
$\frac{\partial}{\partial\omega_0}$	$\frac{X}{\omega}$	$\frac{X(\omega^2+\hat{\omega}_0^2)}{\omega\cdot\hat{\omega}_0^2}-\frac{2\cdot X}{\omega}$	$\frac{2\omega\cdot\hat{\omega}_0}{X(\omega^2+\hat{\omega}_0^2)^2}$

Considering small deviations, errors of the estimations can be approximated with (11)-(13):

$$\left|\frac{\Delta R_s}{R_s}\right| \approx \left|\frac{\partial R_s}{\partial R}\frac{\Delta R}{R_s}\right| + \left|\frac{\partial R_s}{\partial X}\frac{\Delta X}{R_s}\right| + \left|\frac{\partial R_s}{\partial\omega_0}\frac{\Delta\omega_0}{R_s}\right| \quad (11)$$

$$\left|\frac{\Delta R_{ct}}{R_{ct}}\right| \approx \left|\frac{\partial R_{ct}}{\partial R}\frac{\Delta R}{R_{ct}}\right| + \left|\frac{\partial R_{ct}}{\partial X}\frac{\Delta X}{R_{ct}}\right| + \left|\frac{\partial R_{ct}}{\partial\omega_0}\frac{\Delta\omega_0}{R_{ct}}\right| \quad (12)$$

$$\left|\frac{\Delta C_{dl}}{C_{dl}}\right| \approx \left|\frac{\partial C_{dl}}{\partial R}\frac{\Delta R}{C_{dl}}\right| + \left|\frac{\partial C_{dl}}{\partial X}\frac{\Delta X}{C_{dl}}\right| + \left|\frac{\partial C_{dl}}{\partial\omega_0}\frac{\Delta\omega_0}{C_{dl}}\right| \quad (13)$$

Equations (11)-(13) combined with Table I give the expressions for relative errors of parameter estimations due to noise (ΔR and ΔX) as well as limited number of measurement points and error in characteristic frequency estimation ($\Delta\omega_0$):

$$\left|\frac{\Delta R_1}{R_s}\right| \approx \left|\frac{\omega\cdot\Delta R}{\omega R+X\omega_0}\right| + \left|\frac{\omega_0\cdot\Delta X}{\omega R+X\omega_0}\right| + \left|\frac{X\cdot\Delta\omega_0}{\omega R+X\omega_0}\right| \quad (14)$$

$$\left|\frac{\Delta R_{ct}}{R_{ct}}\right| \approx \left|\frac{\Delta X}{X}\right| + \left|-\frac{\Delta\omega_0(\omega^2-\omega_0^2)}{\omega_0(\omega^2+\omega_0^2)}\right| \quad (15)$$

$$\left|\frac{\Delta C_{dl}}{C_{dl}}\right| \approx \left|-\frac{\Delta X}{X}\right| + \left|-\frac{2\cdot\omega_0\cdot\Delta\omega_0}{\omega^2+\omega_0^2}\right| \quad (16)$$

Using expressions (14)-(16) with measurement specifications (measurement error and number of measurement points), it is possible to estimate the behavior of the proposed method with different measurement characteristics. Moreover, it may be seen that different factors have different impact on the estimation of a specific parameter.

III. SIMULATION RESULTS AND DISCUSSION

A. Data generation

Three reference sets of R_s, R_{ct} and C_{dl} parameters (Table II) were arbitrary chosen with standard nominal values. Such approach provides the possibility for later hardware-based experiment with the same configuration. Instead of the characteristic angular frequency (ω_0), it is more convenient to show the characteristic frequency (f_0).

TABLE II
REFERENCE VALUES FOR MODEL PARAMETERS

Network	R_s [Ω]	R_{ct} [Ω]	C_{dl} [nF]	f_0 [kHz]
N_1	510.000	820.000	8.200	23.670
N_2	470.000	1000.000	4.700	33.863
N_3	300.000	910.000	3.300	52.999

The complex impedance data was calculated using Eq. (1) in the frequency range from 1 kHz to 100 kHz. The total number of measurement points was chosen, according to Eq. (10), as N=4951 to ensure that the characteristic frequency is estimated with a relative error lower than 1%. To create more realistic test impedance data, a noise of ±0.05% has been added to these reference values. Values of noise level and frequency range are chosen in compliance with specifications of the available measurement device for hardware-based experiment. Frequency range from 1 kHz to 100 kHz is also common for low-cost and widely used microcontroller-based impedance meters. Nyquist plots of input impedance data are shown in Fig. 3.

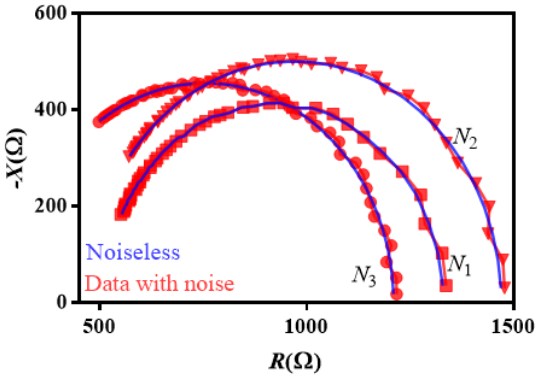

Fig. 3. Nyquist plots of input impedance data

B. Parameter estimation from synthetic data

As a first step in the validation study, the proposed method was applied to the noiseless data. Successively, it was tested with data that contains noise. Our test platform was MATLAB R2013b installed on a Dell notebook with an i7-975H CPU at 2.60 GHz, 16GB of RAM and a 64-bit Windows 10 operating system. The program code used for parameter estimation is provided in Appendix A. Estimated values of model parameters in cases of noiseless and noisy data are shown in Table III and Table IV, respectively.

TABLE III
ESTIMATED VALUES OF MODEL PARAMETERS IN CASE OF NOISELESS DATA WITH N=4951

Network	R_s [Ω]	R_{ct} [Ω]	C_{dl} [nF]	f_0 [kHz]
N_1	510.104	820.128	8.202	23.660
N_2	470.034	1000.014	4.700	33.860
N_3	299.987	910.003	3.300	53.000

TABLE IV
ESTIMATED VALUES OF MODEL PARAMETERS IN CASE OF DATA WITH NOISE WITH N=4951

Network	R_s [Ω]	R_{ct} [Ω]	C_{dl} [nF]	f_0 [kHz]
N_1	508.174	817.790	8.164	23.840
N_2	467.582	999.040	4.677	34.060
N_3	300.771	909.816	3.306	52.920

Bars of relative errors for noiseless data and data with noise are shown in Fig. 4 and Fig. 5, respectively. The main features of our method are great repeatability and reproducibility, since the presented method is not iterative. Therefore, the same results will be obtained with every repeated estimation.

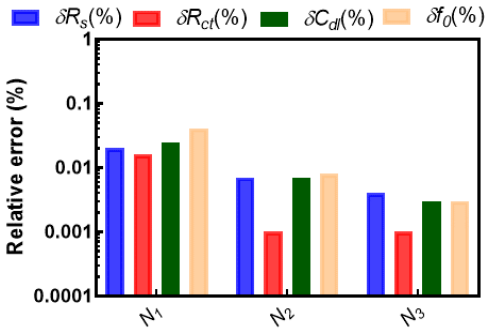

Fig. 4. Relative errors for estimated values in case of noiseless data with 4951 measurement points.

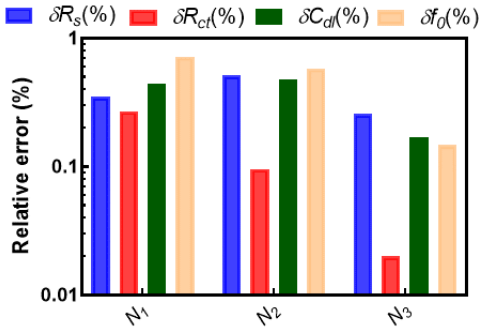

Fig. 5. Relative errors for estimated values in case of data with noise with 4951 measurement points.

With aim to investigate repeatability of the computational performance, simulations were repeated 100 times and average execution times with standard deviations are shown in Fig. 6. As it can be seen from Fig. 6, average execution times were very similar for all tests.

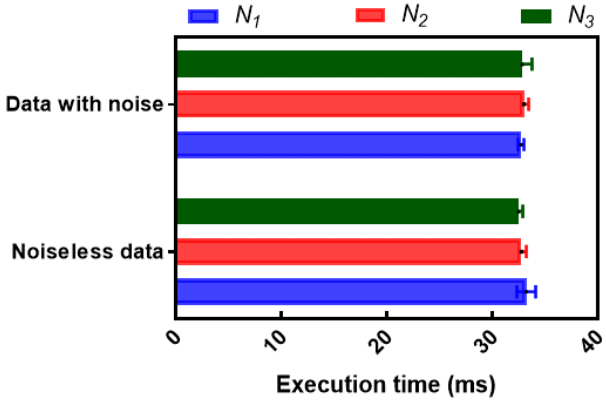

Fig. 6. Average execution times and standard deviations for 100 estimations with 4951 measurement points.

As it can be seen from Fig. 4, characteristic frequencies of all three networks are estimated with relative error lower than 0.05% in the case of noiseless data. All model parameters are estimated with relative errors lower than 0.03%. Moreover, average execution time is very similar for all three networks.

However, when noise is present in impedance data (Fig. 5) characteristic frequencies of all three networks are estimated with relative error lower than 0.720%. Consequently, there are higher relative errors in estimation of model parameters, but still acceptable (lower than 0.520%) for most of the practical applications.

The number of measurement points can be reduced if it is possible to approximately determine the value of characteristic frequency. This can be done in pre-estimation screening (impedance measurement) with a lower number of frequency points. For example, for N_3, if we set 30 kHz instead of 1 kHz in Eq. (10), we obtain that N=166 is needed. Simulations are repeated and obtained results are shown in Table V. Relative errors are shown in Fig. 7.

TABLE V
ESTIMATED VALUES OF MODEL PARAMETERS AND CHARACTERISTIC FREQUENCY WITH N=166

Parameter	Noiseless data	Data with noise
R_s	468.313 Ω	460.934 Ω
R_{ct}	999.331 Ω	996.624 Ω
C_{dl}	4.684 nF	4.616 nF
f_c	34.000 kHz	34.600 kHz

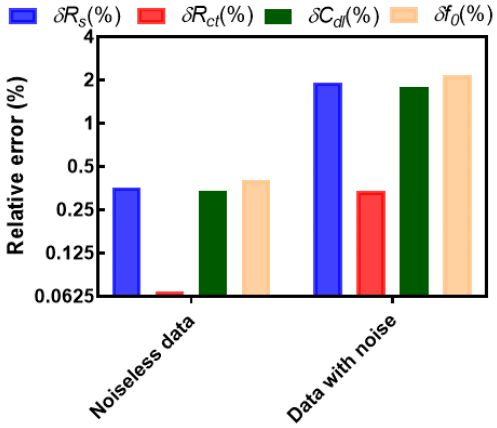

Fig. 7. Relative errors for estimated values in case of noiseless data and data with noise with 166 measurement points.

As it can be seen from Fig. 7, in the case of noiseless data, relative errors are still lower than the defined 1%. Average execution time (100 repetitions) is reduced to 1.183 ms or close to 3.5% of time needed for 4951 measurement points. However, from Table V and Fig. 7 it can be seen that an important aspect must be data pre-processing (filtering) as noise in data increases estimation errors. We will investigate that in a future work.

IV. EXPERIMENTAL RESULTS AND DISCUSSION

A. Parameter estimation from experimentally obtained data in case of discrete components network

We have also analyzed the proposed method with experimentally obtained data. Chemical impedance analyzer IM3590 (Hioki, Japan) was used to measure impedance in the frequency range from 1 kHz to 100 kHz (Fig. 8).

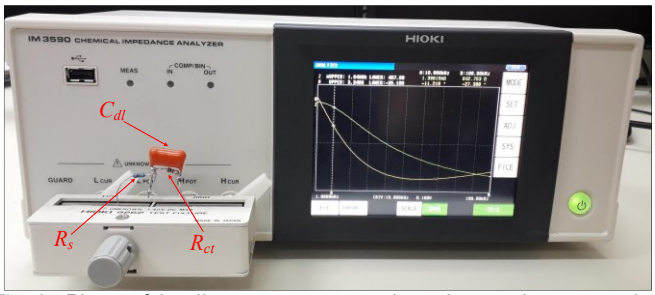

Fig. 8. Photo of the discrete components-based network connected to the measurement device (HOIKI IM3590).

Base error of the model IM3590 is ±0.05% [18]. The electrical network was composed of discrete components whose nominal values equal to the N_2 reference set. However, due to the tolerance of the components we have also measured their resistance and capacitance with Hioki IM3590 in the frequency range from 1 kHz to 100 kHz. Average values are presented as "Measured" in Table VI. As discussed in Section III.B, N=166 was chosen. Estimated values of model parameters and relative errors when compared to the measured values are summarized in Table VI. Relative errors are lower than 1%, which confirms our simulation analysis.

TABLE VI
COMPARISON OF MEASURED, ESTIMATED AND NOMINAL VALUES (ESTIMATION IN MATLAB)

	R_s	R_{ct}	C_{dl}
Nominal	470 Ω±5%	1000 Ω±5%	4.7 nF±10%
Measured	467,121 Ω	985,341 Ω	4.845 nF
Estimated	469.896 Ω	980.804 Ω	4.859 nF
Error	0.594%	-0.460%	0.279%

Fig. 9 shows a comparison of Nyquist plots of measured, estimated and calculated values.

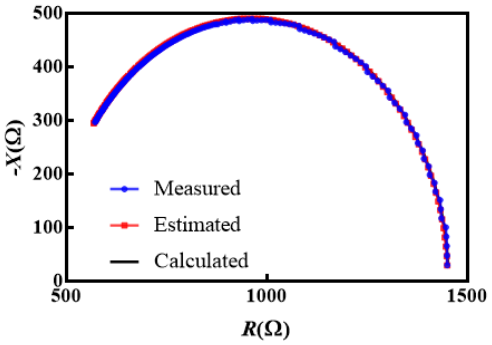

Fig. 9. Nyquist plots of measured, estimated and calculated impedance data

Additional analysis of the proposed method was done with Root Mean Square Error (RMSE) calculations. Obtained values are 2.434 Ω for resistance and 1.6130 Ω for reactance, respectively.

B. Microcontroller-based implementation

As it is mentioned above, the main focus in our study is the development of a low-complexity method that is suitable for implementation in low-priced microcontroller-based portable systems. Our test platform was a microcontroller board based on ATmega2560 microcontroller with available 256 kB of flash memory, 8 kB of SRAM and a clock speed of 16 MHz. The internal analog-to-digital converter is 10-bit, while float variables are 32-bit. The program code written in Arduino IDE for parameter estimation is provided in Appendix B. The same data set used in Section IV.A was uploaded to the microcontroller flash memory. Program code uses 6804 of 253952 bytes (2%) of available flash memory. Global variables use 5003 of 8192 bytes (61%) of SRAM. Obtained results are summarized in Table VII.

TABLE VII
COMPARISON OF MEASURED, ESTIMATED AND NOMINAL VALUES (ESTIMATION WITH MICROCONTROLLER)

	R_1	R_2	C_2
Nominal	470 Ω±5%	1000 Ω±5%	4.7 nF±10%
Measured	467.121 Ω	985.341 Ω	4.845 nF
Estimated	469.90 Ω	980.80 Ω	4.86 nF
Error	0.595%	-0.461%	0.310%

As it can be seen, the same results (as in MATLAB) are obtained using basic mathematical operations available in standard C/C++ compiler for 8-bits microcontrollers. Moreover, when compared to the PC configuration needed for operation on desktop-based software for EIS, implementation of our approach on platforms with low memory and low processing capabilities presents a significant contribution. Additionally, the execution time of 34.096 ms can be considered suitable for many real-time applications.

C. Analytical application #1: Impedance of microfluidic platform for isomalt detection

In our recent study [19], we showed that through impedance measurement between the silver electrodes of a microfluidic platform is possible to detect when isomalt is present in the microfluidic channel. As an additional study, in this paper we analyzed the parameter estimation of the simplified Randles circuit of such an impedance. Impedance measurement was performed with PalmSens4 instrument in 11 points in frequency range 10 kHz-100kHz (Fig. 10).

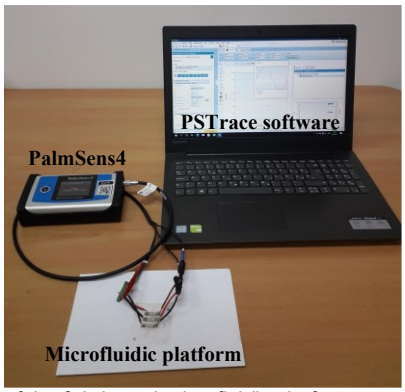

Fig. 10. Photo of the fabricated microfluidic platform connected to the measurement device.

Estimated values of model parameters are shown in Table VIII. A graphical comparison of measured and estimated impedance plots is shown in Fig. 11.

TABLE VIII
ESTIMATED VALUES OF MODEL PARAMETERS WHEN ISOMALT IS INSERTED IN MICROFLUIDIC CHANNEL

R_s [Ω]	R_{ct} [Ω]	C_{dl} [μF]
321.235	14.788	0.433

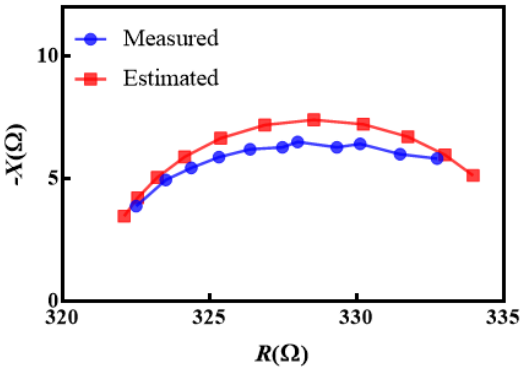

Fig. 11. Nyquist plots of measured and estimated impedance data

Obtained RMSE values are 1.075 Ω for resistance and 0.616 Ω for reactance.

D. Analytical application #2: Impedance of Panasonic 18650PF Li-ion Battery

As it was mentioned above, the Randles circuit is widely used for modelling of various batteries. As a final part of the validation process, we used publicly available dataset of impedance measurements of a brand new 2.9 Ah Panasonic 18650PF cell [20]. Measurements were done in a thermal chamber with Digatron Firing Circuits Universal Battery Tester. We chose measurement ID=3541 from the dataset. The impedance was measured in 12 points within the frequency range from 0.3372 Hz to 8 Hz while the temperature was kept constant at 25 °C. Estimated values of model parameters are shown in Table IX.

TABLE IX
ESTIMATED VALUES OF MODEL PARAMETERS FOR IMPEDANCE OF PANASONIC 18650PF LI-ION BATTERY

R_s [Ω]	R_{ct} [Ω]	C_{dl} [mF]
25.891	31.838	3.546

A graphical comparison of measured and estimated impedance plots is shown in Fig. 12.

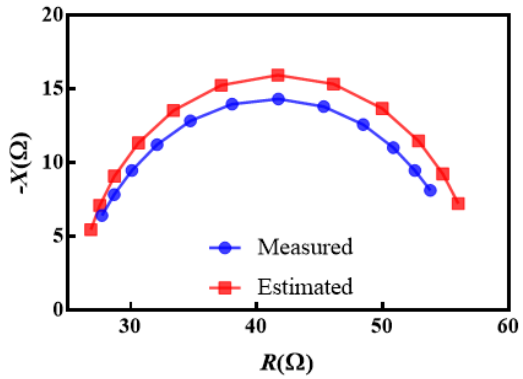

Fig. 12. Nyquist plots of measured and estimated impedance data

Obtained RMSE values are 2.124 Ω for resistance and 0.914 Ω for reactance.

V. CONCLUSION

In this work, we presented a method for parameter estimation of the simplified Randles circuit that is suitable for implementations on low-cost embedded hardware. A deep theoretical, numerical and experimental analysis of the proposed method was performed. It was shown that our approach is not limited for use on PC platforms but can also work on microcontroller-based platforms with standard functions of C/C++ compilers. No single additional library is required. Therefore, our approach is suitable for use on other embedded or portable platforms as well.

Our future work is directed towards realization of the integrated system for impedance measurement and *in-situ* parameter estimation. An important aspect of our future work will be a selectivity study as well. In this paper we applied our estimation method on impedance data with one time constant

(Randles circuit). However, a study with mixed time-constant is also very important for wider use of our method. Moreover, we plan to analyze and implement different digital filters for pre-processing of the measured impedance.

APPENDIX

A. MATLAB implementation

```
clear all
clc
%reference model parameters
R1 = 470;
R2 = 1000;
C2 = 4.7e-9;
%calculation of characteristic frequency
w0=1/(R2*C2);
f0=w0/(2*pi);
%definition of minimum and maximum frequency
fmin = 1e3;
fmax = 1e5;
%number of frequency points
%N = 4951;
N=166;
%create frequency vectors
f=linspace(fmin, fmax, N);
w = 2 * pi * f;
%model of noiseless data
Z = R1 + R2./(1+1i*w*R2*C2);
%noise addition
rng(0,'twister');
a = -0.05;
b = 0.05;
r = (b-a).*rand(N,1) + a;
Z = Z.*(1+0.01*r');
%extract real and imaginary part of impedance
R = real(Z);
X = imag(Z);
%define number of repeats
M=100;
elapsed_time = zeros(M,1) ;  % initialize the
elapsed times
result = zeros(M,1) ;

for j=1:1:M
t = tic ; %start measurement of execution time
[~,idx] = max(abs(X)); %find index of characteristic
frequency
w0_est = w(idx);%estimate w0
f0_est=w0_est/(2*pi);%calculate f0
%estimation of model parameters
for i=1:1:N
R2_est(i) = -(X(i)*(w0_est^2 +
w(i)^2))/(w0_est*w(i));
C2_est(i) = -w(i)/(X(i)*(w0_est^2 + w(i)^2));
R1_est(i) = (w0_est*X(i) + R(i)*w(i))/w(i);
end
 t = toc(t); %stop measurement of execution time
elapsed_time(j) = t; % put execution time of this
iteration in vector
end
time_avg = mean(elapsed_time);%find average
execution time
%print estimated values
fprintf('rel_err(R1) %.3f Mean(R1): %.3f std(R1):
%.3e\n', 100*(mean(R1_est)-R1)/R1, mean(R1_est),
std(R1_est));
fprintf('rel_err(R2) %.3f Mean(R2): %.3f std(R2):
%.3e\n', 100*(mean(R2_est)-R2)/R2, mean(R2_est),
std(R2_est));
fprintf('rel_err(C2) %.3f Mean(C2): %.3e std(C2):
%.3e\n', 100*(mean(C2_est)-C2)/C2, mean(C2_est),
std(C2_est));
fprintf('f0(Hz): %.3f\n', f0_est);
fprintf('rel_err(f0) %.3f\n', 100*(mean(f0_est)-
f0)/f0);
fprintf('Average elapsed time(100 reps) %.4e\n',
time_avg);
%end
```

B. Microcontroller program code

Due to the limited space, just portion of vectors f, R and X are shown. Complete dataset is available upon request.

```
#define N 166
float f[N] ={1000,1600,…, 100000};
float R[N]={1449.689,1449.212, …, 570.003};
float X[N]={-29.986,-47.771,…, -295.398};
float w[N];
int i = 0;
float maxImag = 0.0;
char index = 0;
float Rs_est[N], Rct_est[N], Cdl_est[N];
float w0, f0 = 0;
float Rs_est_alg=0, Rct_est_alg=0, Cdl_est_alg=0;
float sum1 = 0, sum2 = 0, sum3 = 0;
unsigned long duration_alg=0;

void setup()
{
 Serial.begin(9600);
 while (!Serial)
 {
  ;
 }
 Serial.println("*******START*******");
 for(i=0;i<N;i++)
 {
  w[i] = 2.0*22.0*f[i]/7.0;
 }
 duration_alg = micros();
 maxImag=abs(X[0]);
 index = 0;
 for(i=1; i<N; i++)
 if (abs(X[i])>=maxImag)
 {
  maxImag = abs(X[i]);
  index = i;
 }
 f0 = f[index];
 w0 = 2.0*22.0*f0/7.0;
 sum1 = 0;
 sum2 = 0;
 sum3 = 0;
for(i=0;i<N;i++)
{
 Rct_est[i] = -(X[i]*(w0*w0 + w[i]*w[i]))/(w0*w[i]);
 Cdl_est[i] = -w[i]/(X[i]*(w0*w0 + w[i]*w[i]));
 Rs_est[i] = (w0*X[i] + R[i]*w[i])/w[i];
 sum1 += Rs_est[i];
 sum2 += Rct_est[i];
 sum3 += Cdl_est[i];
}
 Rs_est_alg = sum1 / N ;
 Rct_est_alg = sum2 / N ;
 Cdl_est_alg = sum3 / N ;
 duration_alg = micros() - duration_alg;
 Serial.print("Execution time: ");
 Serial.print(duration_alg);
 Serial.println(" us");
 Serial.println("*******Estimated values:*******");
 Serial.print("Rs= ");
 Serial.println(Rs_est_alg);
 Serial.print("Rct= ");
 Serial.println(Rct_est_alg);
```

```
  Serial.print("Cdl= ");
  Serial.print(Cdl_est_alg*1e9);
  Serial.println(" nF");
  Serial.println("*******END*******");
}
void loop()
{
}
```

REFERENCES

[1] S. Nejad, D.T. Gladwin, and D.A. Stone." A systematic review oflumped-parameter equivalent circuit models for real-time estimation of lithium-ion battery states", *Journal of Power Sources*, vol. 316, pp. 183-196, 2016. (doi: 10.1016/j.jpowsour.2016.03.042)

[2] A.J. Fairweather, M.P. Foster, and D.A. Stone, "Modelling of VRLA batteries over operational temperature range using Pseudo Random Binary Sequences," *Journal of Power Sources*, vol. 207, pp. 56-59, 2012. (doi: 10.1016/j.jpowsour.2012.02.024.)

[3] R. D. Anderson, Y. Zhao, X. Wang, X. G. Yang and Y. Li, "Real time battery power capability estimation," *2012 American Control Conference (ACC)*, 2012, pp. 592-597, (doi: 10.1109/ACC.2012.6314892).

[4] R. Ferrero, M. Marracci, M. Prioli, and B. Tellini, "Simplified model for evaluating ripple effects on commercial PEM fuel cell", *International Journal of hydrogen energy*, vol. 37, pp. 13462-13469, 2012. (doi: 10.1016/j.ijhydene.2012.06.036)

[5] Z.-M. Gao, Y.-Y. Liu, F. Lin, L.-H. Dang, L.-J. Wen, "EIS Characteristic under Cathodic Protection and Effect of Applied Cathodic Potential on Surface Microhardness of Q235 Steel", *Int. J. Electrochem. Sci.*, vol. 8, pp. 10446 – 10453, 2013.

[6] M. N. Idris, A. R. Daud, and N. K. Othman, "Electrochemical impedance spectroscopy study on corrosion inhibition of benzyltriethylammonium chloride", *AIP Conference Proceedings*, vol. 1571, no. 23, pp. 23-28, 2013. (doi: 10.1063/1.4858624)

[7] J. Lia, N. Birbilisb, R. G. Buchheita, "Electrochemical assessment of interfacial characteristics ofintermetallic phases present in aluminium alloy 2024-T3", *Corrosion Science*, vol. 101, pp. 155–164, 2015. (doi: 10.1016/j.corsci.2015.09.012)

[8] S. B. Meyer, P. L'Eplattenier, J. Deng, M. Zhu, C. Bae, T. Miller, "Randles Circuit Parameters Set Up for battery Simulations in LS-DYNA", *15th Internalnational LS-DYNA Users Conference*, June 10-12, 2018, Detroit, USA.

[9] J. E. Craven, D. S. Kinnamon and S. Prasad, "Randles Circuit Analysis Toward Investigating Interfacial Effects on Microchannel Electrodes," *IEEE Sensors Letters*, vol. 2, no. 1, pp. 1-4, 2018, (doi: 10.1109/LSENS.2018.2803519).

[10] D. K. Sharma K. Pareek, A. Chowdhury, "Investigation of solar cell degradation using electrochemical impedance spectroscopy", *International Journal of Energy Research*, vol. 44, pp. 8730-8739, 2020. (doi: 10.1002/er.5567)

[11] B. Sanchez, A. S. Bandarenka, G. Vandersteen, J. Schoukens, R. Bragos, "Novel approach of processing electrical bioimpedance data using differential impedance analysis," *Medical Engineering and Physics*, vol. 35, no. 9, pp. 1349–1357, 2013. (doi:10.1016/j.medengphy.2013.03.006)

[12] B. Sanchez, E. Louarroudi, E. Jorge, J. Cinca, R. Bragos, R. Pintelon, "A new measuring and identification approach for time-varying bioimpedance using multisine electrical impedance spectroscopy," *Physiological Measurement*, vol. 34, no. 3, pp. 339–357, 2013. (doi:10.1088/0967-3334/34/3/339)

[13] M. Simić, Z. Babić, V. Risojević, G. M. Stojanović, "Non-iterative parameter estimation of the 2R-1Cmodel suitable for low-costembedded hardware", *Frontiers of Information Technology & Electronic Engineering*, vol. 21, no. 3, pp. 476-490, 2020. (doi: 10.1631/FITEE.1900112)

[14] M. Simić, Z. Babić, V. Risojević, G. M. Stojanović, "A Novel Non-Iterative Method for Real-Time Parameter Estimation of the Fricke-Morse Model", *Advances in Electrical and Computer Engineering*, vol. 16, no. 4, pp. 57-62, 2016. (doi: 10.4316/AECE.2016.04009)

[15] S. Kumar, A. Ghosh and R. Bandyopadhyay, "Parameter Estimation of Randles Model of Electronic Tongue Using System Identification", *2019 IEEE International Symposium on Olfaction and Electronic Nose (ISOEN)*, 2019, pp. 1-4, (doi: 10.1109/ISOEN.2019.8823202).

[16] G. Miramontes-de-León, C. Sifuentes-Gallardo, A. Moreno-Báez, E. García-Domínguez and R. Magallanes-Quintanar, "Time-Frequency Analysis of a Pulsed Excitation and Its Application in Randles Model," *2015 International Conference on Mechatronics, Electronics and Automotive Engineering (ICMEAE)*, 2015, pp. 157-161, (doi: 10.1109/ICMEAE.2015.20).

[17] J. E. B. Randles, "Kinetics of Rapid Electrode Reactions", *Discussions of the Faraday Society*, vol. 1, pp. 11-19, 1947. (doi: 10.1039/df9470100011)

[18] https://www.hioki.com/en/products/detail/?product_key=5749 (Accessed on June 4th, 2021)

[19] G. M. Stojanović, T. Kojić, M. Simić, A. Jovanović-Galović, B. Pavlović, A. Zurutuza, L. Anzi, and R. Sordan, "Rapid selective detection of ascorbic acid using graphene based microfluidic platform", *IEEE Sensors Journal*, vol. 21, no. 15, pp. 16744-16753, 2021. (doi: 10.1109/JSEN.2021.3078692)

[20] P. Kollmeyer, "Panasonic 18650PF Li-ion Battery Data", Mendeley Data, V1, 2018. (doi: 10.17632/wykht8y7tg.1)

Dr. Mitar Simić (S'16, M'18) was born in Ljubovija, Republic of Serbia in 1987. He received the B.Sc. and M.Sc. degrees in electrical engineering from the University of East Sarajevo, Bosnia and Herzegovina, in 2010 and 2012, respectively. He received the Ph.D. degree in electrical engineering from the University of Novi Sad, Serbia in 2017.

He is a Postdoctoral Researcher within the STRENTEX project at the Faculty of Technical Sciences, University of Novi Sad, Serbia.

He is an author/coauthor of one monograph and more than 40 scientific papers. His research interests include sensors, flexible electronics, impedance spectroscopy analysis, equivalent circuit modeling, and development of devices for impedance measurement and data acquisition.

Adrian K. Stavrakis (S'21) was born in Samothraki, Greece, in 1992. He received his B.Sc. degree in Electronics Engineering from the Intenational Hellenic University (ex. named ATEITH) in Thessaloniki Greece in 2016, followed by a postgraduate certification in Smart Systems Integration from Heriot-Watt University in Edinburgh, UK (2018), and a full scholarship under the Erasmus+ scheme for a joint M.Eng. in electrical and optical engineering by Télécom SudParis in France and an M.Sc. in Smart Telecom and Sensing Networks by Aston University, Birmingham, UK (2020).

He is currently pursuing his Ph.D. at the University of Novi Sad, Serbia in the domain of flexible and textile electronics.

His research interests include systems design, simulation and characterization, antennas, remote sensing, electronics, microfluidics, and cross platform integration.

Prof. Dr. Goran Stojanović (M'04) is a full professor at Faculty of Technical Sciences (FTS), University of Novi Sad (UNS), Serbia. He received a BSc, MSc and a PhD degree in 1996, 2003 and 2005, respectively, from FTS-UNS, all in electrical engineering.

He has 25 years of experience in R&D. His research interests include sensors, flexible electronics, textile electronics and microfluidics. He is an author/coauthor of 260 articles, including 96 in leading peer-reviewed journals with impact factors, 5 books, 3 patents, 1 chapter in monograph. Keynote speaker for 12 international conferences. Stojanović has been a supervisor of 11 PhD students, 40 MSc students and 60 diploma students at the FTS-UNS. He has more than 14 years' experience in coordination of EU funded projects (H2020, FP7, EUREKA, ERASMUS, CEI), with total budget exceeding 14.86 MEUR. Currently, he coordinates 4 Horizon2020 projects in the field of green electronics and textile electronics.